ISSN 2829-4998

A compact patch antenna for wireless sensor network applications in WLAN

Md. Firoz Ahmed [a,1,*], Samiul Bashir [a,2], Pronab Kumar Paul [a,3], Md. Bipul Islam [a,4], A.N.M. Shihab Uddin [a,5], M. Hasnat Kabir [a,6]

[a] Department of Information and Communication Engineering, University of Rajshahi, Rajshahi- 6205, Bangladesh
[1] firozice01@gmail.com; [2] samiulprogramming@gmail.com; [3] pronabpual77@gmail.com; [4] bipulice18106@gmail.com;
[5] anmshihabuddin@gmail.com; [6] hasnatkabir11@gmail.com
* corresponding author

ARTICLE INFO

Article history
Received October 11, 2024
Revised November 9, 2024
Accepted December 3, 2024
Available online December 30, 2024

Keywords
Rectangular patch antenna
WSNs
Inset feedline
Partial grounding
WLAN band

ABSTRACT

In wireless sensor networks (WSNs), antennas play a crucial role in enlarging network capacity, prolonging transmission distances, fostering spatial reuse, and minimizing interference. This paper delineates a miniature rectangular patch antenna featuring partial grounding, meticulously engineered for the WLAN (wireless local area network) to promote real-time operations within WSNs. The main goal is to augment the creation and execution of a patch antenna that aligns with the typical size and power constraints of WSN nodes. The antenna is engineered and simulated for a 2.4 GHz WLAN frequency band (2.4 – 2.48 GHz) by leveraging CST Microwave Studio 2024. It is fabricated on a 45 mm × 50 mm FR4 substrate (ε_r = 4.3, thickness = 1.4 mm, loss tangent = 0.025). The antenna is energized via a 50 Ω microstrip inset-feed line. This antenna demonstrates a substantial bandwidth of 159.729 MHz (2.31963 GHz to 2.479359 GHz), an impressive return loss of – 48.15956 dB, a VSWR (voltage standing wave ratio) of 1.007848, a directivity of 4.7 dBi, a gain of 3.04 dBi, and an efficiency of 68.21%. These performance indicators illustrate the antenna's effectiveness in enabling short-range communication within WSNs. With its compact design, broad bandwidth, and strong performance metrics, this antenna serves as an efficient and cost-effective solution suitable for various applications in WSNs, including industrial automation, environmental monitoring, healthcare, and smart city initiatives, thereby ensuring reliable and high-quality wireless communication.

1. Introduction

Wireless sensor networks (WSNs) are essential for monitoring and collecting data from various structures by deploying multiple sensor nodes. These networks heavily rely on efficient and reliable wireless communication between the sensor nodes, which is facilitated by antennas. Patch antennas, known for their compact size and ease of integration, are commonly used in WSNs. However, there are still gaps in the design of patch antennas for WSNs that need to be addressed to enhance their overall performance. These gaps include improving antenna radiation, ensuring acceptable return loss, and minimizing power consumption. Several designs and techniques [1]–[3] have been proposed in the literature to elevate the quality of patch antennas featuring different layouts for WSN fields. One such approach involves the use of Hilbert geometry, which achieves a significant footprint lessening of 77%

https://doi.org/10.3176/aet.v3i3.1702

contrasted to conventional rectangular patch antennas. However, there is still a need for further investigation into the cost, return loss, and energy utilization to ensure the suitability of these antennas for WSNs. In [4], a pioneering wearable antenna functioning at 5 GHz for body-centric wireless sensor networks is introduced. Nonetheless, the antenna's design comprises a regular microstrip patch affixed to a gold substrate, which may adversely influence overall performance and escalate system costs. Furthermore, the antenna design in this investigation is simulated and optimized utilizing computer simulation CST Microwave Studio, which may lead to increased time complexity and potentially constrict the total gain of the antenna. The conception of a dense E-carved microstrip patch antenna for WBANs (wireless body area networks), a CPW (coplanar waveguide)-fed incredibly-broadband antenna for WSNs, and an omni-directional patch antenna has also been advocated to enhance the efficiency of antenna systems [5]–[7]. However, these methodologies predominantly concentrate on low-profile designs and incorporate amended bow-tie-molded vertical patches with uneven ground surfaces, thereby amplifying costs and design intricacies.

A layered patch antenna with double circular polarization is suggested for multiple-input multiple-output (MIMO) wireless local area networks. Utilizing a square ring slot feeding technique, this antenna improves system efficacy concerning cross-polar features and isolation [8]. A pair of L- threaded microstrip patch antenna is evolved for WSN scenarios, where the SLOA (Sea Lion optimization algorithm) is employed to foster antenna performance in sensor nodes [9]. Various designs of frequency reconfigurable antennas, dual-band CPW-fed minuscule planar antennas, and hybrid rectangular circle microstrip antennas alongside flawed ground layouts are presented for wireless services. The focus is on wideband frequency coverage and omni-directional radiation patterns. The designs utilize substrate category FR-4 with a tangent loss of 0.019 and a dielectric permittivity of 4.7. However, these designs may not be the optimum solution for receiving multimedia data in wireless sensor networks for live communication due to their complexity and potential performance limitations [10]. Indeed, the efficacy of the network may be compromised by a broadband microstrip patch antenna that has certain gambling at the V band, which may aggravate total return loss [11]. Wireless sensor networks are not a good fit for a diminutive E-pattern microstrip patch antenna for wireless networks because of the lack of bandwidth [12]. Additionally, a model for a wideband patch antenna with shorting vias is proposed for wideband applications but is limited to TE02 mode propagation and cannot be used for WSN [13].

Through two distinct strategies described in [14], [15], the authors anticipate to raise the patch antenna's spectrum by utilizing the loading degenerate patch paradigm. The aforementioned methods are not feasible for communicating in actual-time in wireless sensor networks, though, because they need the employment of many parasitic patches, which adds to the delay. A compact microstrip patch antenna for wireless sensor nodes was proposed in [16]. Furthermore, a pair of band microstrip patch antenna without misleading signals is suggested to collect energy from radio frequencies [17]. A microstrip ring patch antenna functioning in the X-band was crafted and simulated by implementing Ansys HFSS [18]. This design utilized fixed patch dimensions and dielectric thickness, incorporating Rogers RT-5880 and FR-4 materials. The resulting performance exhibited bandwidths ranging from 260 to 1160 MHz and gains between 4.6 and 9.35 dB. A monopole antenna performing in the 3.43–3.61 GHz frequency spectrum, envisaged for WiMAX purposes, was assembled [19] incorporating a FR4 substrate. However, these studies do not address the monitoring of antenna performance within the sensor node, and more attention is needed in terms of power controlling, emission, and return loss to accomplish the challenges of real-time situations in wireless sensor networks.

This paper presents a novel creation and analysis of a delicate rectangular patch antenna with a partial grounding strategy, foremost tailored for WLAN applications in wireless sensor networks (WSNs). Operating at a frequency of 2.4 GHz, the antenna is optimized for efficient short-range communication, showcasing significant improvements in impedance matching, bandwidth, and gain through its innovative inset-feedline structure. This advancement enhances energy utilization, promoting high-quality data transmission essential for real-time WSN applications. The research highlights key performance parameters like a return loss (–48.15956 dB), a bandwidth (159.729 MHz), and an efficiency (68.21%), making this cost-effective, high-performance antenna ideal for applications in environmental monitoring, healthcare, and smart city initiatives.

2. Method

2.1. Materials

2.1.1. FR-4 Material

Flame Retardant 4 (FR-4) is a widely used material in the crafting of printed circuit boards (PCBs), known for its glass-reinforced epoxy laminate composition. This material excels in providing excellent electrical insulation and mechanical strength, making it highly suitable for various electronic applications. The FR-4 material is composed of fiberglass cloth that has been woven and treated with epoxy resin. Numerous advantageous qualities are imparted by this special mixture, such as reduced water absorption, superior temperature resistance, and great dimensional stability. By adding to FR-4's strength and rigidity, the woven fiberglass reinforcement helps it resist mechanical stress and keeps the PCB from warping or bending. FR-4 is well known for its exceptional electrical characteristics, including a low dissipation factor and excellent dielectric strength, in addition to its mechanical attributes. In order to stop electrical leaks and retain signal integrity in electronic circuits, these qualities guarantee effective insulation. The affordability of FR-4 is one of its key benefits. It is the perfect option for the bulk fabrication of PCBs because it is easily accessible and reasonably priced. Additionally, FR-4 is easy to employ during fabrication because it works with a variety of production techniques, including as soldering, etching, and drilling. Because of its exceptional electrical insulation, mechanical durability, flame-retardant properties, and affordability, FR-4 is a widely used material for PCBs. It guarantees the correct functioning and lifetime of electrical equipment in addition to offering a dependable substrate [20], [21].

2.2. Partial Ground Plane Strategy

The partial ground plane strategy for patch antennas boosts performance and tailors radiation characteristics by modifying a segment of the ground plane instead of requiring a complete redesign. This adjustment may involve the introduction of notches, slots, or various shapes to enhance particular parameters. The advantages of using the partial ground plane approach are notable: it enables beam steering, directing energy to targeted regions; allows for polarization control to easily switch between linear and circular polarization; facilitates size reduction by trimming the ground plane; and increases bandwidth through optimized impedance matching. Designing an antenna that utilizes the partial ground plane Strategynecessitates meticulous analysis and modeling with specialized software to fulfill specific performance criteria and application needs [22]–[25].

2.3. Inset-Feedline Strategy

The inset-fed line technique is widely recognized as an effective tactic for feeding patch antennas. This method works by leveraging a microstrip transmission line attached to the identical substrate as the patch. The inset-fed line, a slender strip of conductive material such as copper, is strategically positioned along the edge of the antenna. It creates an electromagnetic field that facilitates the transfer of energy into the antenna. By fine-tuning parameters such as width, length, and inset distance, designers can optimize impedance matching and enhance radiation characteristics. This technique is advantageous due to its simplicity, efficient impedance control, customizable radiation patterns, and compact design, making it ideal for applications with limited space. Achieving optimal performance and impedance matching requires meticulous design and simulation [26]–[29].

2.4. Antenna Structure and Design

Three essential elements for attaining optimal performance in the construction of a rectangular patch antenna are the substrate's height (h), frequency of operation (f_r), and dielectric constant (ε_r).

- Dielectric Constant of the Substrate ($\boldsymbol{\varepsilon_r}$): The efficacy of the antenna is greatly influenced by the dielectric constant (ε_r) of the substrate material. A lesser ε_r value corresponds to elevated radiation efficiency, wider radiation patterns, lower conductor losses, and greater bandwidth. In contrast, an increased ε_r value leads to a reduction in the dimensions of the antenna patch. The chosen substrate material, FR4 lossy, features a dielectric constant (ε_r) of 4.3. This value falls within the typical range of 2.2 to 12 commonly found in microstrip patch antennas [30].
- Operational Frequency ($\mathbf{f_r}$): Antenna performance and efficiency are greatly impacted by the resonance frequency (f_r), which is crucial to their operation [31]. Within the WLAN frequency range of 2.4 to 2.48 GHz, choosing a resonance frequency of 2.4 GHz offers a number of advantages, including improved antenna efficacy, system efficiency, and signal integrity.
- Dielectric Substrate Height (**h**): The dielectric substrate height (h) has a considerable effect on several antenna performance factors, including bandwidth, surface wave properties, radiation efficiency, inadvertent feed radiation, and the total antenna size [32]. A substrate height of 1.4 mm has been chosen for the antenna under consideration in order to maximize bandwidth and enable efficient wideband operation. A higher substrate height, however, could present several difficulties, including increased surface wave energy, decreased radiation efficiency, and more fictitious feed radiation. To create an antenna that is small, effective, and performs well, it is crucial to strike a harmonious balance between these factors.

2.5. Design Equations

The schematic equations for the suggested antenna are outlined in [33], [34]:

2.5.1. Step 1: Calculating the patch's width (***W***)

The following equation is implemented to figure out the microstrip patch antenna's width (W):

$$W = \frac{c}{2f_r\sqrt{\frac{(\varepsilon_r - 1)}{2}}} \tag{1}$$

Where, c is the speed of light in a vacuum, or around 3 × 108 m/s, f_r is the resonance frequency, and ε_r is the substrate's dielectric constant.

When employing the aforementioned equation to calculate the width of the patch, it is essential to consider both the resonance frequency and the dielectric properties of the substrate material. The width of the antenna plays a significant role, as it influences the radiation pattern, bandwidth, and resonant frequency. Designers must carefully choose the optimal width to guarantee the antenna operates at the intended frequency, which is vital for fulfilling the anticipated requirements of wireless communication.

2.5.2. Step 2: Height of the substrate($\boldsymbol{h}$)

The width (W) of a microstrip patch antenna must be considerably wider than the substrate's thickness (h) in order for it to radiate effectively and function properly. This idea is commonly stated in the following form:

$$W/_h > 1 \tag{2}$$

To provide the highest potential radiation effectiveness, this requirement ensures that the patch's width is substantially bigger than the substrate's thickness.

2.5.3. Step 3: Effective dielectric constant ($\boldsymbol{\varepsilon_{reff}}$)

A crucial factor to consider when designing microstrip patch antennas is the effective dielectric (ε_{reff}). This parameter takes into account the fringing fields that extend beyond the boundaries of the dielectric substrate, giving the impression that the antenna has a larger size than its actual physical dimensions. This component becomes highly important when the substrate is relatively thick in comparison to the wavelength or has a low dielectric constant. The following formula is utilized to compute the effective dielectric constant.

$$\varepsilon_{reff} = \frac{\varepsilon_r+1}{2} + \frac{\varepsilon_r-1}{2}[1 + 12\frac{h}{w}]^{-\frac{1}{2}} \tag{3}$$

2.5.4. Step 4: The patch's length ($\boldsymbol{L}$)

A microstrip patch antenna's patch length (L) is a critical component that influences the antenna's overall performance as well as its resonant frequency. To calculate this length, the effective length (L_{eff}) and the additional length due to fringing effects (ΔL) must be considered.

$$\boldsymbol{L = L_{eff} - 2\Delta L} \tag{4}$$

Where:

$$\boldsymbol{L_{eff}} = \frac{c}{2f_r\sqrt{\varepsilon_{reff}}} \tag{5}$$

The formula for ΔL, which represents the length extension caused by fringing fields, is:

$$\Delta L = 0.412h\frac{(\varepsilon_{reff}+0.3)(\frac{W}{h}+0.264)}{(\varepsilon_{reff}-0.258)(\frac{W}{h}+0.8)} \tag{6}$$

The dielectric constant and the patch's shape are both included in the effective length (L_{eff}). The extra length brought about by the bordering fields at the patch's edges is explained by the expression 2ΔL. To accurately determine the antenna's resonance frequency, this adjustment is necessary. Usually, simulation software or empirical equations that account for the substrate material and patch size are used to determine L_{eff} and ΔL

2.5.5. Step 5: Substrate length ($\boldsymbol{L_s}$) and Substrate width ($\boldsymbol{W_s}$) = width ($\boldsymbol{W_g}$) and length ($\boldsymbol{L_g}$) of the Ground plane

Because they have a major impact on achieving optimal efficiency, the diameters of the ground plane and substrate are important considerations in antenna design, particularly for microstrip patch antennas. The substrate influences the electromagnetic properties of the antenna in addition to providing mechanical stability. The ground plane's dimensions serve as the basis for the formulas used to determine the substrate's length (L_S) and width (W_S). The measurements in question are as follows:

$$L_s = L_g = L + 6h \quad (7)$$

$$W_s = W_g = W + 6h \quad (8)$$

These formulas ensure that the ground plane and substrate are the right sizes to provide a strong base and efficient grounding for the antenna. As a result, its operating parameters—such as gain, bandwidth, and radiation efficiency—are improved.

2.5.6. Step 6: A rectangular patch antenna's inset feedline dimensions

To calculate the dimensions of the inset feedline, specifically its length and width, for a rectangular patch antenna, the following formulas can be applied:

- Inset Feedline Width ($\boldsymbol{W_f}$):

  The formula used to calculate the width of the inset feedline is as follows:

$$\boldsymbol{W_f = \frac{W}{2\sqrt{2}}} \quad (9)$$

Where,

W = width of the patch antenna

- Inset Feedline Length ($\boldsymbol{L_f}$):

  The calculation for the length of the inset feedline is determined as follows:

$$\boldsymbol{L_f = \frac{L}{\pi} arcsin\left(\frac{W_f}{W}\right)} \quad (10)$$

Where,

L = the patch antenna's length.

W_f = inset feedline width

- Inset Distance ($\boldsymbol{y_0}$):

  The distance from the outer boundary of the patch to the point where the inset feedline joins (y_0) is:

$$\boldsymbol{y_0 = \frac{W-W_f}{2}} \quad (11)$$

Where,

W = width of the patch antenna

W_f = inset feedline width

These equations are essential for establishing the placement and size of the inset feedline. Their significance lies in their influence on achieving optimal impedance matching between the feedline and the patch. Efficient impedance matching is critical as it reduces signal reflections and enhances power transfer, thereby ensuring that the antenna performs effectively at the targeted resonant frequency.

2.6. Proposed Antenna Configuration

The antenna design illustrated in Fig. 1 comprises several essential elements: a FR4 dielectric substrate, a rectangular patch, a PGP (partial ground plane), and a carefully crafted 50-Ohm inset feedline aimed at optimizing performance. The structure is built on an FR4 substrate, a material widely utilized in printed circuit boards (PCBs). This FR4 dielectric substrate features a loss tangent ($tan\ \delta$) of 0.025 and a dielectric constant (ε_r) of 4.3. It measures 45 mm by 50 mm ($L_s \times W_s$) and a thickness (h) of 1.4 mm and is positioned directly above the ground plane. The antenna includes a rectangular patch, serving as the radiating component, measuring 28.65 mm by 36.65 mm ($L \times W$). This patch is situated over a partial ground plane that measures 45 mm by 34 mm ($L_g \times W_g$), providing an efficient return path for electromagnetic currents. The ground plane's design aids in trimming the total area of the antenna while enhancing its radiation properties. Both the patch and the ground plane are constructed from annealed copper, with a uniform thickness (t) of 0.035 mm. The choice of copper ensures excellent electrical conductivity, minimizing signal attenuation and energy loss.

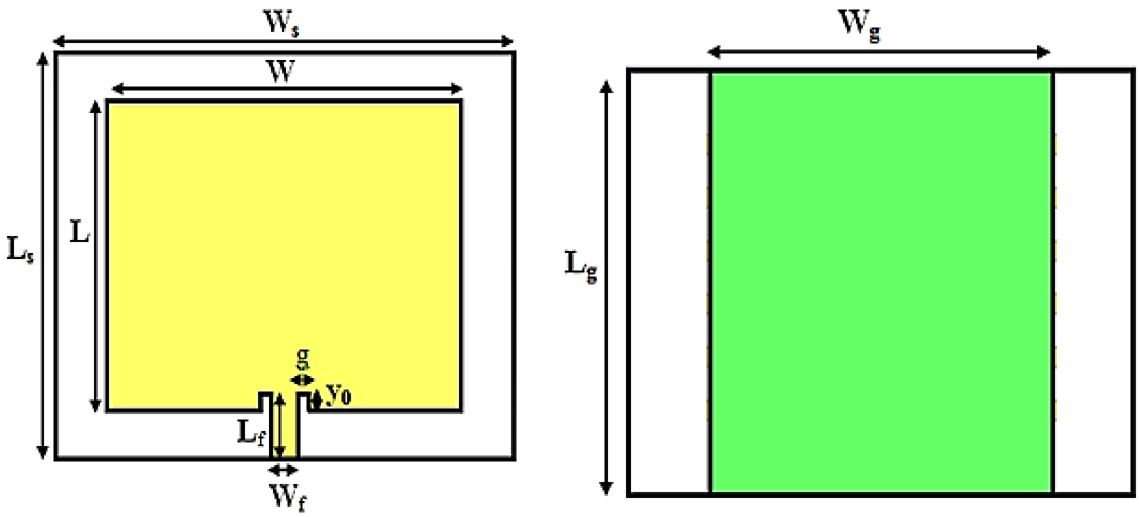

(a) (b)

Fig. 1. Layout of the proposed antenna design featuring a partial ground plane: (a) Front perspective and (b) Rear perspective

An inset feedline of 50 Ohms connects the patch to the external circuitry. This feedline measures 9.48 mm by 3.137 mm ($L_f \times W_f$) and features an inset gap (g) of 1 mm and an inset distance (y_0) of 1.3 mm. This configuration is designed to align the impedance of the patch with that of the external circuitry, facilitating optimal power transfer and reducing signal reflections. The aggregate sizes of the proposed antenna, as defined in Table 1, have been meticulously optimized for efficient operation within the targeted frequency band, specifically for WLAN applications operating at the 2.4 GHz frequency. Computer Simulation Technology (CST) Microwave Studio software 2024 was utilized to establish the design parameters, guaranteeing that the finished product complies with the specified WLAN usage criteria.

Table 1. Geometric features of the suggested antenna design being evaluated

No.	Parameters	Value
1.	Frequency band used	WLAN
2.	Operating frequency, f_r (GHz)	2.4
3.	Dielectric constant of the substrate, ε_r	4.3
4.	Thickness of the substrate, h	1.4 mm
5.	Length of the substrate, L_s	45 mm
6.	Width of the substrate, W_s	50 mm
7.	Width of the partial ground, W_g	34 mm
8.	Length of the ground plane, L_g	45 mm
9.	Length of the patch, L	28.65 mm
10.	Width of the patch, W	36.65 mm
11.	Thickness of the copper, t	0.035 mm
12.	Width of the feed, W_f	3.137 mm
13.	Feed length, L_f	9.48 mm
14.	Inset distance, y_0	1.3 mm
15.	Inset gap, g	1 mm
16.	Characteristics impedance of feedline (Z_0)	50 Ω

3. Results and Discussion

This section offers a thorough examination of the intended antenna structure's effectiveness traits as derived from simulations conducted employing Computer Simulation Technology (CST) Microwave Studio software 2024 at 2.4 GHz. The simulation outcomes yield essential insights into the antenna's effectiveness, emphasizing seven critical metrics: return loss, bandwidth, voltage standing wave ratio (VSWR), directivity, radiation pattern, gain, and efficiency. Together, these metrics provide a thorough grasp of the antenna's capabilities and its potential applicability across different scenarios.

3.1. Return Loss (S11)

Return loss (S_{11}) quantifies the energy bounces off to the source due to mismatched impedance between the antenna and its feedline, and it is defined in decibels (dB). A lesser return loss value signifies superior impedance matching, resulting in a more effective transfer of power. Typically, a $S_{11}<-10$ dB is deemed acceptable for a well-engineered antenna, indicating that over 90% of the power is successfully radiated. Conversely, high return loss values are unfavorable as they reflect poor impedance matching, leading to substantial power reflection and diminished efficiency.

Fig. 2 portrays the return loss (S_{11}) characteristics of the suggested antenna. The S_{11} in the envisaged antenna design measures –48.15956 dB at the 2.4 GHz resonant frequency. This measurement exemplifies exceptional impedance matching, greatly exceeding the standard threshold of –10 dB. Such a low return loss indicates that only about 0.01% of the incident power is reflected, with approximately 99.99% of the energy being effectively absorbed or transmitted by the antenna. This translates to minimal energy loss and optimal signal radiation. The remarkable return loss of –48.15956 dB underscores the efficacy of the proposed antenna design, representing a significant improvement compared to previous research findings [12], [34], which likely exhibited higher return loss values. This performance is especially beneficial for reliable communication systems functioning in the 2.4 GHz frequency band, encompassing technologies like WiFi (2.4 – 2.48 GHz), Bluetooth (2.4 – 2.485 GHz), ISM Band (2.4 – 2.5 GHz), 4G LTE (2.3 – 2.315 GHz), microwave ovens (2.4 – 2.48 GHz), S-Band

(2.3 – 2.4 GHz), RFID (2.4 – 2.5 GHz), Wireless Communication Services (WCS) (2.345 – 2.360 GHz), and WiMAX (2.3 – 2.4 GHz).

The outstanding return loss achieved by the proposed antenna not only reflects its efficient power utilization but also enhances performance for real-time data transmission and reception. This makes the antenna exceptionally suitable for applications that demand reliable communication and data integrity, outperforming prior designs in both effectiveness and reliability. The minimal energy reflection attained through superior impedance matching ensures that the antenna can deliver robust and stable signal coverage, which is vital for modern wireless communication systems.

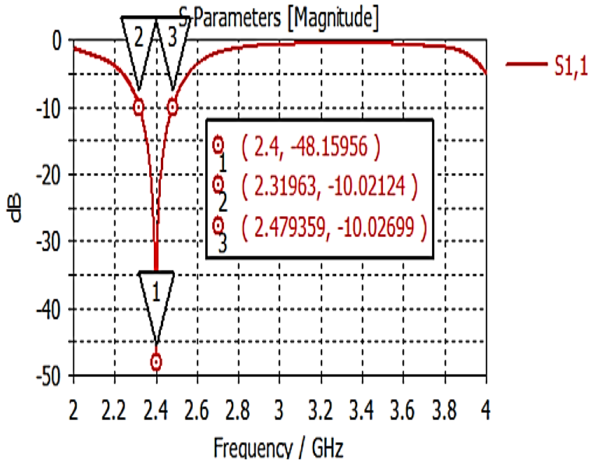

Fig. 2. Return loss (S_{11}) features of the designed antenna

3.2. Antenna's bandwidth

An antenna's bandwidth is the range of frequencies where it operates at its best; it is often indicated by a return loss of lesser than -10 dB, which enables efficient energy transfer. In wireless sensor networks (WSNs) designed for WLAN applications, having a wide bandwidth is essential for accommodating various communication systems and adjusting to different environmental conditions. The antenna proposed in this research, illustrated in Fig. 2, achieves a bandwidth of 159.729 MHz (2.31963 GHz - 2.479359 GHz) at the -10 dB limit, representing a notable advancement compared to earlier designs [12]. This elevated bandwidth enables the antenna to function proficiently over a larger spectrum of frequencies, significantly boosting its reliability and adaptability for WLAN applications within WSNs.

3.3. Voltage Standing Wave Ratio (VSWR)

The Voltage Standing Wave Ratio (VSWR) measures how efficiently an antenna's impedance matches that of its transmission line. VSWR is determined by comparing the upper and lower voltage levels along the transmission line, a phenomenon resulting from the interplay between incident and reflected waves. A VSWR of 1 signifies optimal impedance matching, meaning that all energy from the source is efficiently delivered to the antenna without any reflections. Conversely, as VSWR values rise, they reflect increasingly poor impedance matching, which can lead to greater power reflections and diminished efficiency. Elevated VSWR readings point to subpar matching, which can result in reflections, signal loss, and impairment in the antenna's entire efficacy. The antenna under consideration achieves an impressive VSWR of 1.007848 at the 2.4 GHz resonant frequency, as illustrated in Fig. 3. This performance exceeds findings from earlier studies [12]. With a VSWR closely approaching 1, this result indicates exceptional impedance matching between the transmission line and the antenna at the designated frequency, ensuring that nearly all the energy is supplied to the antenna while minimizing signal loss from reflections.

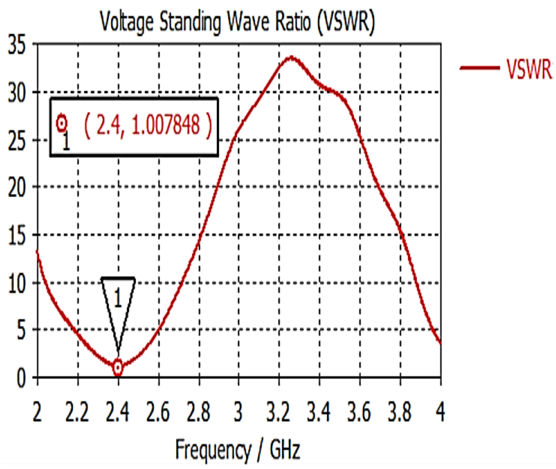

Fig. 3. Voltage Standing Wave Ration (VSWR) characteristics of the suggested antenna

3.4. Gain

The gain of an antenna indicates how effectively it converts input power into radio waves in a specific direction, compared to an isotropic antenna. In wireless sensor networks (WSNs) for WLAN applications, gain plays a crucial role in boosting signal strength and extending communication range. The suggested antenna attains a gain of 3.04 dBi at the 2.4 GHz resonant frequency, as underscored in Fig. 4.

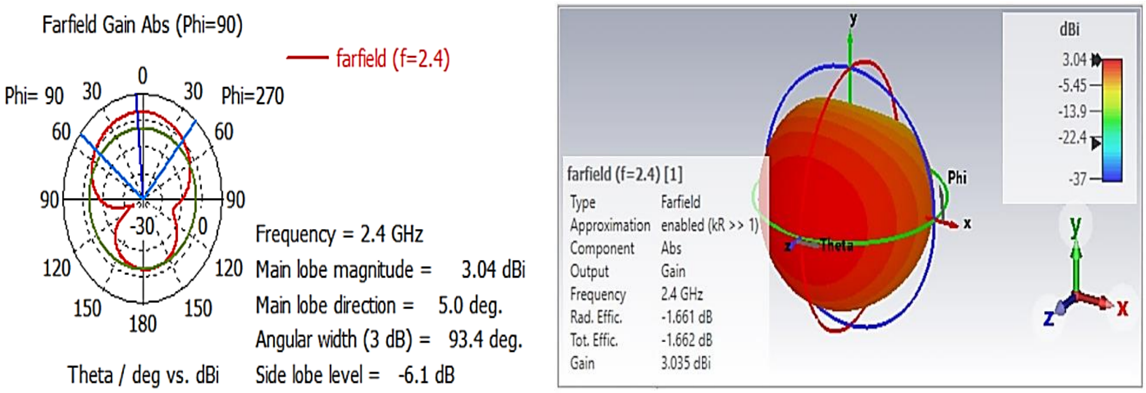

(a) (b)

Fig. 4. 2D and 3D far-field gain graph of the designed antenna

This gain surpasses previously reported performance metrics [34] demonstrating the antenna may properly strengthen the signal in the intended direction. Consequently, the antenna enhances overall network performance by ensuring stronger and more reliable connections between sensor nodes. The 3.04 dBi gain makes this antenna suitable for both indoor and outdoor WSN applications, where consistent and robust signal coverage is essential.

3.5. Directivity

Antenna directivity refers to the propensity of an antenna to concentrate its emitted energy in a specific manner, as opposed to an isotropic antenna that distributes energy uniformly across all angles.

In wireless sensor networks (WSNs) utilizing WLAN technology, directivity plays a vital role in enhancing signal strength, extending communication ranges, and minimizing interference by directing energy exactly where it is most needed. The suggested antenna achieves a directivity of 4.7 dBi at 2.4 GHz, as depicted in Fig. 5.

This level of directivity strikes a favorable balance between targeted energy transmission and wide coverage, making the antenna adaptable to various WSN applications. By funneling more power into specific areas, the antenna enhances communication efficiency, resulting in stronger connections among sensor nodes while still maintaining extensive area coverage. This reliability and effectiveness make the antenna an excellent choice for ensuring robust WLAN performance in WSNs, whether in indoor settings such as smart homes or in expansive outdoor environments.

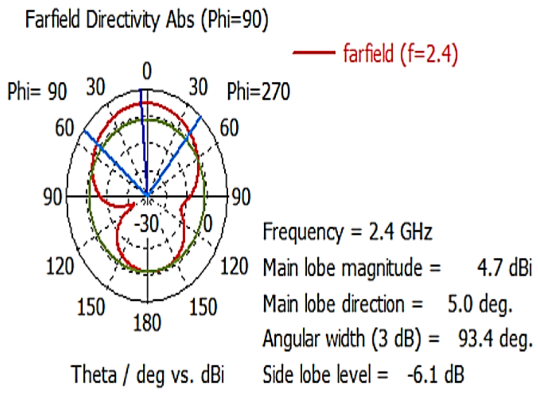

(a)

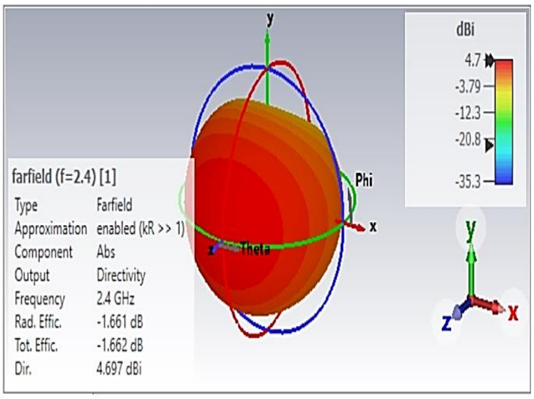

(b)

Fig. 5. 2D and 3D far-field directivity graph of the designed antenna

3.6. Efficiency

The capability of an antenna to transform the energy input into radiated energy while taking losses from heat, mismatched impedances, and other sources into consideration is gauged by its efficiency. High efficiency is essential for maximizing signal strength and minimizing energy loss in wireless local area network (WLAN) sectors in wireless sensor networks (WSNs). The antenna outperforms previous research with an efficiency of 68.21% [12]. This remarkable efficiency level implies that the antenna radiates a good portion of the input power, which elevates network performance and reliability in WSN situations.

3.7. Radiation Pattern

The antenna radiation pattern refers to how an antenna emits energy in different directions, which is crucial for understanding its coverage and performance in wireless sensor networks (WSNs) for WLAN applications.

3.7.1. E-field Pattern

The far-field E-field radiation pattern of the designed antenna for 2.4 GHz, as laid out in Fig. 6(a), exhibits a main lobe magnitude of 17.8 dB (V/m), with the predominant direction of radiation occurring at 0 degrees. This indicates that the antenna has a strong radiation in this direction, making it particularly effective for applications requiring targeted communication. The 3D plot in Fig. 6(b) further confirms that the maximum radiation intensity (Emax) is 17.8 dB (V/m), illustrating the antenna's efficiency in emitting electromagnetic energy in the intended direction.

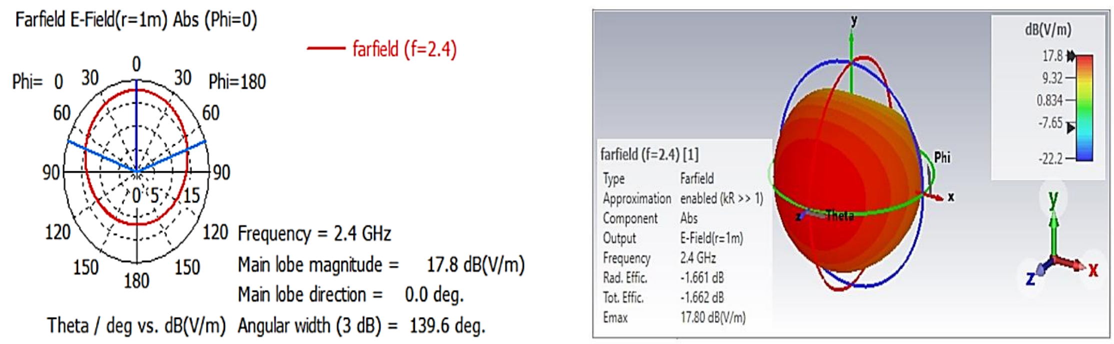

(a) (b)

Fig. 6. The planned antenna's 2D and 3D E-field emission patterns

3.7.2. H-field Pattern

A major lobe magnitude of -37.9 dB (A/m) is made clear by the far-field H-field radiation pattern at 2.4 GHz, which is shown in Fig. 7(a). The main radiation is aimed at 4 degrees. This dB value is negative, which means that the magnetic field is weaker than the electric field, as is typical with patch antennas as the electric field is stronger. The directional magnetic field distribution of the antenna is shown by the 3D figure in Fig. 7(b), which shows that the maximum radiation intensity (Hmax) reaches -33.7 dB (A/m).

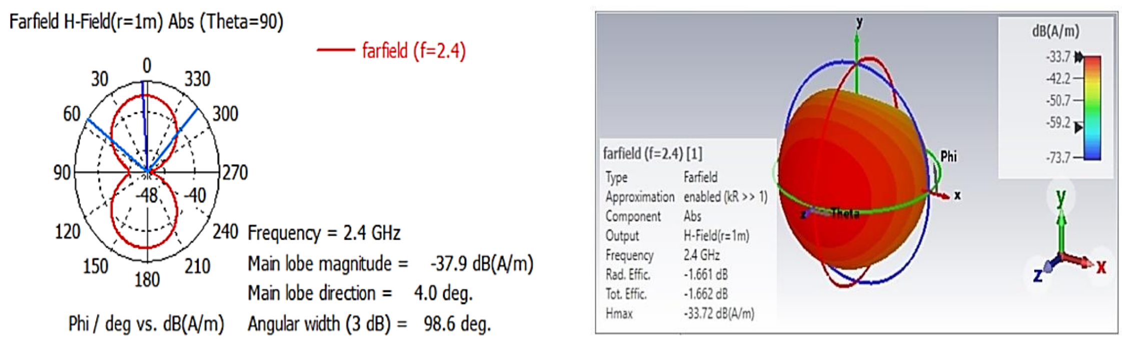

(a) (b)

Fig. 7. Radiation patterns of the designed antenna in both 2D and 3D H-field configurations

The patterns of the electric (E-field) and magnetic (H-field) fields reveal that the antenna possesses distinct and strong directionality in its radiation, which is advantageous for wireless sensor network (WSN) applications. This directionality ensures that the antenna can effectively target specific areas, optimizing signal distribution and minimizing interference, which is crucial for maintaining reliable communication in WSNs.

3.8. Overview of the Simulated Outcomes

The simulated findings shown in Table 2 validate that the suggested antenna design is exceptionally pertinent for WLAN tasks in wireless sensor networks functioning at the 2.4 GHz resonant frequency. With its outstanding impedance matching, wide bandwidth, adequate gain, precise directivity, and high efficiency, this antenna emerges as a dependable and effective option for real-time operations within wireless sensor networks. These attributes guarantee that the antenna provides robust, stable, and efficient wireless communication, which is paramount for the successful implementation of WSNs (wireless sensor networks) across diverse environments.

Table 2. Overview of the outcomes obtained from the suggested antenna design

No.	Metrics of Performance	Proposed Antenna
1.	f_r (Resonant frequency)	2.4 GHZ
2.	S_{11}(Return loss)	–48.15956 dB
3.	Voltage Standing Wave ratio (VSWR)	1.007848
4.	Impedance Bandwidth	159.729 MHz
5.	Gain	3.04 dBi
6.	Directivity	4.7 dBi
7.	efficiency	68.21%

The simulation results affirm the robust performance of the proposed antenna for WLAN-based Wireless Sensor Networks (WSNs) operating at 2.4 GHz. Key metrics include an impressive return loss of – 48.15956 dB, a wide bandwidth of 159.729 MHz, a VSWR of 1.007848, a gain of 3.04 dBi, directivity of 4.7 dBi, and an efficiency of 68.21%. Nevertheless, some limitations exist, such as its relatively modest gain, which may not meet the requirements for long-range applications, as well as performance variability influenced by specific environmental factors. Future endeavors should aim to enhance the gain, broaden the bandwidth, and optimize the design for a wider range of operational frequencies. Furthermore, the fabrication and testing of the antenna under real-world conditions will be essential to validate the simulation results and evaluate its effectiveness across various WSN applications.

3.9. Comparision

The proposed antenna design is evaluated against previous works to emphasize its advancements for WLAN applications in wireless sensor networks (WSNs), as summarized in Table 3. The intended antenna, with dimensions of 45 × 50 × 1.4 mm³, showcases a notable reduction in size compared to earlier designs, such as those in references [12] and [34]. It achieves a superior return loss of –48.15956 dB, an excellent VSWR of 1.007848, and a broader bandwidth of 159.729 MHz, surpassing the performance of previous models. Although its gain of 3.04 dBi is slightly lower than the 6.66 dBi observed in [12], the proposed antenna compensates with improved efficiency of 68.21%, which is higher than the 41.773% efficiency noted in [12]. Overall, the proposed design offers a more compact size, enhanced bandwidth, and better efficiency, making it a significant advancement for WLAN applications in WSNs where efficiency, size, and bandwidth are crucial factors.

Table 3. Comparisons between current and previous works

No.	Ref. No's.	Antenna Dimensions (mm³)	RL (dB)	VSWR	B.W (MHz)	G (dBi)	η (%)
1.	[14] (2022)	60 × 65× 1.6	– 13.89	1.50	64.7	6.66	41.77
2.	[38] (2022)	100 × 100 × 8	–24.50	....	....	2.92	....
3.	Proposed Antenna	45 × 50 × 1.4	–48.15956	1.0078	159.729	3.04	68.21

[a] Note: Ref. No's. = References Number, RL = Return Loss, B.W = Bandwidth, G = Gain,
[b] η = Efficiency

4. Conclusion

In this research, a compact rectangular patch antenna with an inset-fed line and partial grounding operating at the 2.4 GHz WLAN frequency band has been successfully developed and analyzed for real-time wireless sensor network (WSN) uses. The antenna showed significant improvements in return loss, bandwidth, efficiency, directivity, and gain, making it a robust solution for applications requiring proximity to users. Its manageable size, low production cost, and adaptability to the WLAN frequency spectrum highlight its practicality and effectiveness. The improved performance metrics confirm that the antenna is well-suited for reliable wireless communication in various WSN scenarios, delivering high-quality output in real-time applications. Future work will involve fabricating and testing the antenna to compare its simulated and real-world performance. Additionally, efforts will be directed at improving the antenna's gain and expanding its operational frequency ranges to better accommodate a wider spectrum of communication needs and enhance its overall performance in evolving WSN applications.

Acknowledgment

The successful completion of this research and the preparation of this journal article would not have been achievable without the invaluable support, guidance, and encouragement from numerous individuals and entities. I would like to extend my heartfelt gratitude to the Department of Information and Communication Engineering, as well as the professors, for their insightful guidance and unwavering support throughout the research process.

Declarations

Author contribution. As the main writers of this paper, each author contributed equally. The final manuscript has been examined and endorsed by each author.
Funding statement. The authors would like to clarify that they have not obtained any financial support, grants, or funding from any organization, institution, or funding agency for this research.
Conflict of interest. The authors declare no conflict of interest.
Additional information. No additional information is available for this paper.

References

[1] A. S. Elkorany *et al.*, "Implementation of a Miniaturized Planar Tri-Band Microstrip Patch Antenna for Wireless Sensors in Mobile Applications," *Sensors*, vol. 22, no. 2, p. 667, Jan. 2022, doi: 10.3390/s22020667.

[2] A. A. Salih and M. S. Sharawi, "A Dual-Band Highly Miniaturized Patch Antenna," *IEEE Antennas Wirel. Propag. Lett.*, vol. 15, pp. 1783–1786, 2016, doi: 10.1109/LAWP.2016.2536678.

[3] Z. Liang, J. Liu, Y. Li, and Y. Long, "A Dual-Frequency Broadband Design of Coupled-Fed Stacked Microstrip Monopolar Patch Antenna for WLAN Applications," *IEEE Antennas Wirel. Propag. Lett.*, vol. 15, pp. 1289–1292, 2016, doi: 10.1109/LAWP.2015.2505091.

[4] W. Farooq, M. Ur-Rehman, Q. H. Abbassi, Xiaodong Yang, and K. Qaraqe, "Design of a finger ring antenna for wireless sensor networks," in *2016 10th European Conference on Antennas and Propagation (EuCAP)*, Apr. 2016, pp. 1–4, doi: 10.1109/EuCAP.2016.7481827.

[5] U. Afruz and M. A. Kabir, "Design of Compact E-Shaped Microstrip Patch Antenna for Wireless Body Area Network," in *2022 International Conference on Innovations in Science, Engineering and Technology (ICISET)*, Feb. 2022, pp. 157–162, doi: 10.1109/ICISET54810.2022.9775820.

[6] R. Azim, M. T. Islam, H. Arshad, M. M. Alam, N. Sobahi, and A. I. Khan, "CPW-Fed Super-Wideband Antenna With Modified Vertical Bow-Tie-Shaped Patch for Wireless Sensor Networks," *IEEE Access*, vol. 9, pp. 5343–5353, 2021, doi: 10.1109/ACCESS.2020.3048052.

[7] M. T. Islam, A. T. Mobashsher, and N. Misran, "Coplanar Waveguide Fed Printed Antenna with Compact Size for Broadband Wireless Applications," *J. Infrared, Millimeter, Terahertz Waves*, vol. 31, no. 12, pp. 1427–1437, Dec. 2010, doi: 10.1007/s10762-010-9728-7.

[8] E. Zhang, A. Michel, M. R. Pino, P. Nepa, and J. Qiu, "A Dual Circularly Polarized Patch Antenna With High Isolation for MIMO WLAN Applications," *IEEE Access*, vol. 8, pp. 117833–117840, 2020, doi: 10.1109/ACCESS.2020.3004895.

[9] R. George and T. Anita Jones Mary, "Design of Directional Two L shaped Microstrip Patch Antenna for WSN Applications Using Sea Lion Optimization Algorithm," in *2021 International Conference on Advances in Electrical, Computing, Communication and Sustainable Technologies (ICAECT)*, Feb. 2021, pp. 1–6, doi: 10.1109/ICAECT49130.2021.9392454.

[10] M. M. Alam, R. Azim, N. M. Sobahi, A. I. Khan, and M. T. Islam, "A dual-band CPW-fed miniature planar antenna for S-, C-, WiMAX, WLAN, UWB, and X-band applications," *Sci. Rep.*, vol. 12, no. 1, p. 7584, May 2022, doi: 10.1038/s41598-022-11679-7.

[11] N. H. Biddut, M. E. Haque, and N. Jahan, "A Wide Band Microstrip Patch Antenna Design Using Multiple Slots at V-Band," in *2022 International Mobile and Embedded Technology Conference (MECON)*, Mar. 2022, pp. 113–116, doi: 10.1109/MECON53876.2022.9751951.

[12] M. S. Rana and M. M. Rahman, "Study of Microstrip Patch Antenna for Wireless Communication System," in *2022 International Conference for Advancement in Technology (ICONAT)*, Jan. 2022, pp. 1–4, doi: 10.1109/ICONAT53423.2022.9726110.

[13] X. Chen and H. Dou, "Wideband Patch Antenna with Shorting Vias," *Int. J. Antennas Propag.*, vol. 2022, no. 1, pp. 1–11, Apr. 2022, doi: 10.1155/2022/2578409.

[14] K. Da Xu, H. Xu, Y. Liu, J. Li, and Q. H. Liu, "Microstrip Patch Antennas With Multiple Parasitic Patches and Shorting Vias for Bandwidth Enhancement," *IEEE Access*, vol. 6, pp. 11624–11633, Jan. 2018, doi: 10.1109/ACCESS.2018.2794962.

[15] J. Wu, Y. Yin, Z. Wang, and R. Lian, "Broadband Circularly Polarized Patch Antenna With Parasitic Strips," *IEEE Antennas Wirel. Propag. Lett.*, vol. 14, pp. 559–562, 2015, doi: 10.1109/LAWP.2014.2373823.

[16] R. Ramly, A. A. B. Sajak, H. Dao, and M. F. A. Zuhairi, "Design of a compact microstrip patch Antenna for wireless sensor nodes," *J. Eng. Sci. Technol.*, vol. 16, no. 3, pp. 2518–2527, 2021, [Online]. Available at: https://jestec.taylors.edu.my/Vol 16 issue 3 June 2021/16_3_47.pdf.

[17] P. Chindhi, H. P. Rajani, and G. Kalkhambkar, "A Spurious Free Dual Band Microstrip Patch Antenna for Radio Frequency Energy Harvesting," *Indian J. Sci. Technol.*, vol. 15, no. 7, pp. 266–275, Feb. 2021, doi: 10.17485/IJST/v15i7.2025.

[18] M. Hacımehmet, "X band microstrip ring patch antenna design and performance evaluation according to feeding types," *Pamukkale Univ. J. Eng. Sci.*, vol. 28, no. 2, pp. 215–221, Apr. 2022, doi: 10.5505/pajes.2021.30632.

[19] A. H. Yüzer and C. Şeker, "4G C-Shaped compact microstrip antenna design and production," *Pamukkale Univ. J. Eng. Sci.*, vol. 23, no. 5, pp. 532–535, 2017, doi: 10.5505/pajes.2017.27880.

[20] S. J. Ahmad, M. M. Ahmed, and I. Unissa, "Optimization of Environmental Data to Improve Safety in Coal Mine using Wireless Sensor Networks," *Indian J. Sci. Technol.*, vol. 15, no. 19, pp. 956–964, May 2022, doi: 10.17485/IJST/v15i19.686.

[21] Q. Wang, Y. Jiang, and Y. Wang, "Novel FR4-based low loss reconfigurable filter with four operating modes using movable transmission lines," *Microw. Opt. Technol. Lett.*, vol. 66, no. 5, p. e34171, May 2024, doi: 10.1002/mop.34171.

[22] R. S. A. Anooz and B. K. Ammar, “A Modified Ground for Bandwidth Enhancement of the Microstrip Patch Antenna for 5G Wireless Communications,” *Int. J. Electr. Electron. Eng.*, vol. 11, no. 2, pp. 19–23, Feb. 2024, doi: 10.14445/23488379/IJEEE-V11I2P103.

[23] A. A. Deshmukh, S. Surendran, A. Rane, Y. Bhasin, and V. A. P. Chavali, “Compact designs of circular microstrip antennas employing modified ground plane for wideband response,” *AEU - Int. J. Electron. Commun.*, vol. 176, p. 155130, Mar. 2024, doi: 10.1016/j.aeue.2024.155130.

[24] H. S. Rajappa, D. N. Chandrappa, and R. Soloni, “Partial Ground-Based Miniaturized Ultra Wideband Microstrip Patch Antenna,” *Indian J. Sci. Technol.*, vol. 17, no. 2, pp. 105–111, Jan. 2024, doi: 10.17485/IJST/v17i2.2622.

[25] I. Jayasukumari, G. Themozhi, and C. Amali, “Investigation and Compatibility of a Low Profile Wideband Circular Ring Patch Antenna with Slotted Partial Ground Plane,” in *Advances in Science and Technology*, Sep. 2023, vol. 130, pp. 137–141, doi: 10.4028/p-xSqy7p.

[26] M. I. Hossain, M. N. Islam, M. A. Islam, and M. T. Ahmed, “Minaret Shape Micro-Strip Patch Antenna with Partial Ground Plane for Lower 5G and Wi-Max Applications,” *J. Digit. Integr. Circuits Electr. Devices*, vol. 8, no. 2, pp. 10–18, Aug. 2023, doi: 10.46610/JDICED.2023.v08i02.002.

[27] K. S. Praveena and M. P. Chandrashekar, “Performance evaluation of inset feed microstrip patch antenna parameters with different substrate materials for 5G wireless applications,” *Radioelectron. Comput. Syst.*, vol. 2024, no. 4, pp. 141–155, Nov. 2024, doi: 10.32620/reks.2024.4.12.

[28] M. Alaba, D. B. Onyango Konditi, and V. K. Oduol, “Inset-fed microstrip patch antenna optimization for 2.4 GHz using surrogate model assisted differential evolution machine learning algorithm,” *Indones. J. Electr. Eng. Comput. Sci.*, vol. 36, no. 2, p. 901, Nov. 2024, doi: 10.11591/ijeecs.v36.i2.pp901-912.

[29] G. P. Raj and K. N. Ketavath, “Dual-band inset-fed diamond-shaped patch MIMO antenna for wireless communication applications,” *Phys. Scr.*, vol. 99, no. 8, p. 085546, Aug. 2024, doi: 10.1088/1402-4896/ad624d.

[30] A. Bansal and R. Gupta, “A review on microstrip patch antenna and feeding techniques,” *Int. J. Inf. Technol.*, vol. 12, no. 1, pp. 149–154, Mar. 2020, doi: 10.1007/s41870-018-0121-4.

[31] J. V. Kumar and S. M. Shaby, “Optimizing inset-fed rectangular micro strip patch antenna by improved particle swarm optimization and simulated annealing,” *Netw. Comput. Neural Syst.*, pp. 1–31, May 2024, doi: 10.1080/0954898X.2024.2358961.

[32] S. Dase and I. Razak, “Optimization of an inset-fed calculations for rectangular microstrip antenna,” *Comput. Sci. Inf. Technol.*, vol. 4, no. 2, pp. 143–148, Jul. 2023, doi: 10.11591/csit.v4i2.p143-148.

[33] F. Ahmed, H. Kabir, and T. Islam, “Design of a compact patch antenna with bandwidth and efficiency improvement for UWB applications,” *Multidiscip. Sci. J.*, vol. 5, no. 4, p. 2023030, May 2023, doi: 10.31893/multiscience.2023030.

[34] M. Benzaghta, B. Er, G. Bilgin, E. Aydin, And A. Kara, “A Miniaturized Multi-layer Microstrip Antenna for Linear Wireless Sensor Network Monitoring Systems,” *Gazi Univ. J. Sci.*, vol. 35, no. 3, pp. 875–884, Sep. 2022, doi: 10.35378/gujs.962910.